

Transport processes in the gravitational collapse of an anisotropic fluid

J. Martínez

*Statistical Physics Group, Physics Department, Faculty of Sciences, Building Cc,
Universidad Autónoma de Barcelona, 08193, Bellaterra, Barcelona, Spain*

(Received 14 November 1995)

In this paper we introduce a method to study the influence of thermal conduction and viscous processes in a spherically symmetric gravitational collapse. We assume that the viscosity appears because of the interaction between the neutrinos and the matter that composes the fluid. The temperature, bulk viscous pressure, and shear viscous pressure are found. The effect of the latter in the anisotropy of the fluid is studied as well. To this end it is necessary to solve two sets of partial differential equations. First, the Einstein equations are solved using the seminumerical HJR method. The causal Maxwell-Cattaneo-type transport equations form the second set of equations to be solved. The temperature profile, found from the heat transport equation, indicates that the energy of the neutrinos in the surface is not correlated with that of the interior. This behavior, which can be explained in terms of the Eddington approximation, allows us to estimate the thickness of the neutrinosphere. The contribution of the shear viscous pressure to the anisotropy in the core of the star is found to be non-negligible. [S0556-2821(96)03512-6]

PACS number(s): 04.25.Dm, 05.70.Ln, 97.60.-s

I. INTRODUCTION

The physical study of relativistic stars usually rests on the assumption of local isotropy. However, at least for high densities, theoretical evidence suggests that this may not be a very accurate approximation [1–3]. Then, it seems fitting to adopt anisotropic models to carry out a more detailed analysis of the relativistic collapse of neutron stars arising from supernovae explosions. The presence of radiation flow during the collapse reveals the existence of anisotropy in the fluid even in the diffusion approximation. Effectively, if the radiation is in this approximation, it interacts strongly with matter, and the interchange of momentum between the different layers of the star will enhance viscous processes. Therefore, because of the presence of a shear viscous pressure, the fluid must be treated as locally anisotropic. On the opposite limit (free streaming) one has anisotropy associated with the direction of propagation of the radiation. Because of this, it is suitable to introduce an anisotropic state equation if one wishes to analyze systems in which the flow of radiation non-negligibly influences the dynamics of the collapse [4–6].

We shall adopt the seminumerical method of Herrera, Jiménez, and Ruggeri (HJR) [7] to solve the Einstein equations. Furthermore, to find the temperature and bulk and shear viscous pressure it will be necessary to introduce a set of transport equations. To solve them we will adopt the explicit expressions for the transport coefficients of heat conductivity and bulk and shear viscosity of an interacting mixture of matter and radiation found by Weinberg [8]. This requires us to determine which reactions are more relevant in the momentum transport between the different star layers. The large neutrino mean free path implies high transport coefficients. Thus, viscous processes induced by interactions between neutrinos and matter are much more important than those induced by other scattering processes. The cooling by absorption and emission of neutrinos drive the star to equilibrium. Among the sources of neutrino opacities it seems that

the scattering with electrons ($e^- + \nu \rightarrow e^- + \nu$) and nucleon absorption ($\nu + n \rightarrow e^- + p$) may account for this process [9–12].

The temperature is a key quantity to decide which processes can take place during the collapse. Moreover it is indispensable to calculate the bulk and shear viscous pressure. Unluckily the solution of the Einstein equations does not provide any information about it. This is why a set of transport equations must be adopted. The standard Eckart theory of irreversible processes [13–15] exhibits undesirable effects (i.e., it predicts an infinite speed of propagation for thermal and viscous signals and unstable equilibrium states). It is then necessary to resort to another thermodynamic theory of irreversible processes that does not present this anomalous behavior. The *extended irreversible thermodynamics* (EIT) theory [16,17] seems to be a good candidate to replace the old Eckart theory and it has been used in cosmological problems with good results [18–20]. Essentially the EIT rests on two hypotheses: (1) The dissipative flows (heat flow and viscous pressures) are considered as independent variables; hence, the entropy function depends not only on the classical variables (particle number and energy density) but on these dissipative flows as well. (2) At equilibrium state, the entropy function is a maximum. Moreover, its flow depends on all dissipative flows and its production rate is semipositive definite. As a consequence the heat flow \mathcal{Q}^μ , the bulk viscous pressure Π , and the traceless viscous tensor $\pi_{\mu\nu}$ obey the evolution equations [21]

$$\tau_{\mathcal{Q}} \dot{\mathcal{Q}}^\nu h_\nu^\mu + \mathcal{Q}^\mu = \chi h^{\mu\nu} [T_{,\nu} - T \dot{U}_\nu - T(\alpha_0 \Pi_{,\nu} - \alpha_1 \Pi_{\nu,\rho}^\rho)],$$

$$\tau_{\Pi} U^\alpha \Pi_{,\alpha} + \Pi = -\zeta U_{;\mu}^\mu + \alpha_0 \zeta \mathcal{Q}_{;\mu}^\mu,$$

and

$$\tau_{\pi} \dot{\pi}_{\mu\nu} + \pi_{\mu\nu}$$

$$= 2\eta \sigma_{\mu\nu} - 2\eta \alpha_1 \mathcal{Q}_{\alpha;\beta} \left(h_{(\mu}^\alpha h_{\nu)}^\beta - \frac{1}{3} h_{\mu\nu} h^{\alpha\beta} \right),$$

respectively, where $\tau_{\mathcal{Q}}$, τ_{Π} , and τ_{π} are the relaxation time of thermal, bulk viscous, and shear viscous signals, respec-

tively. T stands for the temperature, χ for the thermal conductivity coefficient, and ζ and η for the bulk and shear viscous coefficients, respectively. The parameters α_0 and α_1 are connected with the characteristics of the fluid under study. The spatial projector tensor is designed by $h_{\mu\nu} = g_{\mu\nu} - U_\mu U_\nu$, and $\sigma_{\mu\nu} = U_{(\mu;\nu)} - \dot{U}_{(\mu} U_{\nu)} - h_{\mu\nu} U_{;\mu}^\mu/3$ is the shear tensor. Here, the overdot denotes $\dot{A}_{\alpha\beta\dots} = U^\lambda A_{\alpha\beta\dots;\lambda}$. It can be seen that if some reasonable assumptions are met, these equations preserve the causality condition and predict stable equilibrium configurations [22]. However, the transport equations for the dissipative flows predicted by EIT are extremely involved. Nevertheless, in the linear approximation the evolution equations for dissipative flows reduce to

$$\begin{aligned}\tau_Q \dot{Q}^\nu h_\nu^\mu + Q^\mu &\simeq \chi h^{\mu\nu} [T_{,\nu} - T \dot{U}_\nu], \\ \tau_\Pi U^\alpha \Pi_{,\alpha} + \Pi &\simeq -\zeta U_{;\mu}^\mu,\end{aligned}$$

and

$$\tau_\pi \dot{\pi}_{\mu\nu} + \pi_{\mu\nu} \simeq 2\eta \sigma_{\mu\nu},$$

which are the covariant formulations of Maxwell-Cattaneo transport equations [23,24]. One may hope that the propagation speed of the dissipative signals is comparable to the sound velocity. For this to be true the relaxation time in the transport equations must be nearly the radiation mean free time. After calculating the temperature we shall obtain both the bulk and shear viscous pressures, which cannot be directly found from Einstein equations. In this way we will establish the influence of shear viscous pressure on the anisotropy of the system.

The paper is organized as follows. In Sec. II the Einstein equations, for an anisotropic sphere composed by a mixture of radiation and matter, are derived, and we resort to the HJR method to solve them. In Sec. III we write the Maxwell-Cattaneo transport equations within the HJR formalism and find the mean free path of the neutrinos as a function of the temperature. This is applied to a specific case in Sec. IV. As an initial configuration, we shall adopt the anisotropic static solution of Gokhroo and Mehra [25]. This one corresponds to an anisotropic fluid with variable energy density. Lastly, Sec. V summarizes the results of this work.

We adopt metrics of signature -2 . The quantities subscripted with a denote that they are evaluated at the surface of the star. The subscripts 0 and 1 indicate partial differentiation with respect to time (u) and radial coordinate (r), respectively, finally an overdot on scalar quantities means d/du . A caret over a quantity means that this one is measured by a Minkowskian observer comoving with the fluid.

II. FIRST SET OF EQUATIONS: EINSTEIN FIELD EQUATIONS

A. Interior and exterior metrics

Our aim is to describe a nonstatic spherically symmetric fluid distribution. To this end we adopt the radiation coordinates [26,27], then the interior metric takes the form

$$ds^2 = e^{2\beta} \left[\frac{V}{r} du^2 + 2dudr \right] - r^2 (d\theta^2 + \sin^2\theta d\phi^2), \quad (2.1)$$

where $u = x^0$ is a timelike coordinate, $r = x^1$ is the null coordinate and $\theta = x^2$ and $\phi = x^3$ are the usual angle coordinates. The u coordinate is the retarded time in flat space-time and, therefore, the u -constant surfaces are null cones open to the future. The metric functions β and V in Eq. (2.1) are functions of u and r . A function $\tilde{m}(u, r)$ can be defined by

$$V = e^{2\beta} [r - 2\tilde{m}(u, r)], \quad (2.2)$$

which is the generalization, inside the distribution, of the ‘‘mass aspect’’ defined by Bondi *et al.* [26]. In the static limit it coincides with the Schwarzschild mass.

In order to give a clear physical meaning to the above formulas, we introduce local Minkowskian coordinates (t, x, y, z) related to Bondi’s radiation coordinates by

$$dt = e^\beta \left(\sqrt{\frac{V}{r}} du + \sqrt{\frac{r}{V}} dr \right), \quad (2.3)$$

$$dx = e^\beta \sqrt{\frac{r}{V}} dr, \quad (2.4)$$

$$dy = r d\theta, \quad (2.5)$$

$$dz = r \sin\theta d\phi, \quad (2.6)$$

and to the Schwarzschild coordinates (T, R, Θ, Φ) by

$$T = u + \int_0^r \frac{r}{V} dr, \quad (2.7)$$

$$R = r, \quad \Theta = \theta, \quad \Phi = \phi. \quad (2.8)$$

Outside matter the metric is the Vaidya one [28], a particular case of the Bondi metric in which $\beta = 0$ and $V = r - 2m$.

B. Stress-energy tensor

As we mentioned above we consider an anisotropic fluid sphere composed by a material medium plus radiation. The material medium travels in the radial direction with a velocity ω in a Minkowski coordinate system. The radiation is treated in the diffusive regime because it interacts strongly with matter. Because of this interaction, viscous processes appear. Thus, a viscous term must be considered in the stress-energy tensor. We denote this term by $\hat{T}_{\mu\nu}^V$ and, for a local Minkowskian observer comoving with the fluid, it can be written as

$$\hat{T}_{\mu\nu}^V = \hat{\tau}_{\mu\nu} = \hat{\pi}_{\mu\nu} + \Pi \hat{h}_{\mu\nu}, \quad (2.9)$$

where $\hat{\pi}_{\mu\nu}$ denotes the traceless viscous pressure tensor, $\hat{h}_{\mu\nu} = \eta_{\mu\nu} - \hat{U}_\mu \hat{U}_\nu$ the spatial projection tensor, and Π is the bulk viscous pressure. For this comoving observer \hat{U}_μ complies with $\hat{U}_\mu = \delta_\mu^t$, and applying the condition $\hat{\pi}_{\mu\nu} \hat{U}^\mu = 0$ together with traceless character of $\hat{\pi}_{\mu\nu}$, we obtain

$$\hat{\pi}_{\mu\nu} = \begin{pmatrix} 0 & 0 & 0 & 0 \\ 0 & \pi & 0 & 0 \\ 0 & 0 & -(\pi/2) & 0 \\ 0 & 0 & 0 & -(\pi/2) \end{pmatrix}. \quad (2.10)$$

Not all anisotropies can be explained in terms of the interaction between matter and radiation. Therefore, it is necessary to bear in mind that the material part of the stress-energy tensor must reflect the anisotropic character of the fluid. For the Minkowskian observer the anisotropic material part of the stress-energy tensor $\hat{T}_{\mu\nu}^M$ is given by the expression

$$\hat{T}_{\mu\nu}^M = (\rho_M + P_t) \hat{U}_\mu \hat{U}_\nu - P_t \eta_{\mu\nu} + (P - P_t) \hat{\chi}_\mu \hat{\chi}_\nu, \quad (2.11)$$

where $\hat{\chi}_\mu = \delta_\mu^x$, ρ_M denotes the material energy density, P the material pressure, and $P_t = P + \rho$ the material part of the tangential pressure. Thus, the pressure ρ refers to the anisotropies that cannot be explained as a result of the matter-radiation interaction.

The last term in the stress-energy tensor accounts for the presence of radiation. In the *Lagrangian frame* (the *proper frame*) and in the diffusive regime it reads [29,30]

$$\hat{T}_{\mu\nu}^R = \begin{pmatrix} \rho_R & -\mathcal{Q} & 0 & 0 \\ -\mathcal{Q} & \mathcal{P} & 0 & 0 \\ 0 & 0 & \mathcal{P} & 0 \\ 0 & 0 & 0 & \mathcal{P} \end{pmatrix}, \quad (2.12)$$

where ρ_R denotes the radiation energy density, \mathcal{Q} the heat flow, and \mathcal{P} the radiation pressure.

Thus, for a local observer comoving with matter, with radial velocity ω , the stress-energy tensor in local Minkowskian coordinates is

$$\hat{T}_{\mu\nu} = \hat{T}_{\mu\nu}^M + \hat{T}_{\mu\nu}^R + \hat{T}_{\mu\nu}^V,$$

and in virtue of (2.9)–(2.12) it can be written as

$$\hat{T}_{\mu\nu} = (\rho + P_\perp) \hat{U}_\mu \hat{U}_\nu - P_\perp \eta_{\mu\nu} + (P_r - P_\perp) \hat{\chi}_\mu \hat{\chi}_\nu + 2 \hat{\mathcal{Q}}_{(\mu} \hat{U}_{\nu)}, \quad (2.13)$$

with

$$\hat{U}_\mu = (1, 0, 0, 0), \quad (2.14)$$

$$\hat{\chi}_\mu = (0, 1, 0, 0), \quad (2.15)$$

$$\hat{\mathcal{Q}}_\mu = \mathcal{Q}(0, -1, 0, 0), \quad (2.16)$$

$$\rho = \rho_M + \rho_R, \quad (2.17)$$

$$P_r = P + \mathcal{P} + \Pi + \pi, \quad (2.18)$$

and

$$P_\perp = P_r - \frac{3}{2} \pi + \rho. \quad (2.19)$$

The physical variables (energy density ρ , radial pressure P_r , tangential pressure P_\perp , and heat flow \mathcal{Q}) are obtained as measured by the mentioned observer, and the effects of gravitation are clearly provided through the appropriate transformation to a curvilinear coordinate system.

To study the dynamics of the system (i.e., ω) it is necessary to obtain the stress-energy tensor as seen by an observer at rest with respect to the Minkowskian coordinates. To this end it is necessary to apply a Lorentz boost in the radial direction to $\hat{T}^{\mu\nu}$. A further transformation allows us to express the stress-energy tensor in curvilinear coordinates (see [6] for details). Thus, applying a local coordinate transformation (2.3)–(2.6) and a Lorentz boost in the radial direction to (2.13) we obtain the stress-energy tensor

$$T_{\mu\nu} = (\rho + P_\perp) U_\mu U_\nu - P_\perp g_{\mu\nu} + (P_r - P_\perp) \chi_\mu \chi_\nu + 2 \mathcal{Q}_{(\mu} U_{\nu)}, \quad (2.20)$$

as measured by an observer using Bondi coordinates with a radial velocity, with respect to the matter configuration, $-\omega$. After performing the transformation, expressions (2.14)–(2.16) read

$$U_\mu = e^\beta \left(\sqrt{\frac{V}{r}} \frac{1}{(1-\omega^2)^{1/2}}, \sqrt{\frac{r}{V}} \left(\frac{1-\omega}{1+\omega} \right)^{1/2}, 0, 0 \right), \quad (2.21)$$

$$\chi_\mu = e^\beta \left(-\sqrt{\frac{V}{r}} \frac{\omega}{(1-\omega^2)^{1/2}}, \sqrt{\frac{r}{V}} \left(\frac{1-\omega}{1+\omega} \right)^{1/2}, 0, 0 \right), \quad (2.22)$$

and

$$\mathcal{Q}_\mu = -\mathcal{Q} \chi_\mu. \quad (2.23)$$

Note that $\mathcal{Q}^\mu U_\mu = 0$ and $\mathcal{Q} = \sqrt{-\mathcal{Q}^\mu \mathcal{Q}_\mu}$.

Applying these transformations to the traceless viscous tensor (2.10), we get

$$\pi_{\mu\nu} = \begin{pmatrix} e^{2\beta} \frac{V}{r} \left(\frac{\omega^2}{1-\omega^2} \right) \pi & -e^{2\beta} \left(\frac{\omega}{1+\omega} \right) \pi & 0 & 0 \\ -e^{2\beta} \left(\frac{\omega}{1+\omega} \right) \pi & e^{2\beta} \frac{r}{V} \left(\frac{1-\omega}{1+\omega} \right) \pi & 0 & 0 \\ 0 & 0 & -\frac{r^2}{2} \pi & 0 \\ 0 & 0 & 0 & -\frac{r^2 \sin^2 \theta}{2} \pi \end{pmatrix}. \quad (2.24)$$

Outside matter the stress-energy tensor corresponds to that of a null fluid: i.e.,

$$T^{\mu\nu} = \varepsilon k^\mu k^\nu, \quad (2.25)$$

where

$$k^\mu = \delta_r^\mu e^{-2\beta} \sqrt{\frac{V}{r}}. \quad (2.26)$$

C. Einstein field equations

Inside matter the Einstein field equations, $G_{\mu\nu} = 8\pi T_{\mu\nu}$, can be written as

$$\begin{aligned} & \frac{1}{4\pi r(r-2\tilde{m})} [-\tilde{m}_0 e^{-2\beta} + (1-2\tilde{m}/r)\tilde{m}_1] \\ & = \frac{1}{1-\omega^2} (\rho + 2\omega Q + P_r \omega^2), \end{aligned} \quad (2.27)$$

$$\frac{\tilde{m}_1}{4\pi r^2} = \frac{1}{1+\omega} [\rho - Q(1-\omega) - P_r \omega], \quad (2.28)$$

$$\beta_1 \frac{r-2\tilde{m}}{2\pi r^2} = \frac{1-\omega}{1+\omega} (\rho - 2Q + P_r), \quad (2.29)$$

$$\begin{aligned} & -\frac{\beta_{01} e^{-2\beta}}{4\pi} + \frac{1}{8\pi} \left(1 - 2\frac{\tilde{m}}{r}\right) \left(2\beta_{11} + 4\beta_1^2 - \frac{\beta_1}{r}\right) \\ & + \frac{3\beta_1(1-2\tilde{m}_1) - \tilde{m}_{11}}{8\pi r} = P_\perp, \end{aligned} \quad (2.30)$$

while outside matter, the only nonvanishing Einstein equation yields

$$\tilde{m}_0 = -4\pi r^2 \varepsilon \left(1 - \frac{2\tilde{m}(u)}{r}\right). \quad (2.31)$$

To algebraically solve the physical variables present in the above set of field equations (2.27)–(2.30) we must find out both β and \tilde{m} . The HJR method will help us in this task, but before it we must impose the junction conditions between exterior and interior metrics.

D. Junction conditions and surface equations

The mass function can be expressed as

$$\tilde{m} = \int_0^r 4\pi r^2 \tilde{\rho} dr. \quad (2.32)$$

It involves an effective energy density given by the right-hand side of (2.28):

$$\tilde{\rho} = \frac{1}{1+\omega} [\rho - Q(1-\omega) - P_r \omega], \quad (2.33)$$

which in the static limit reduces to the energy density of the system.

From (2.29) one has

$$\beta = \int_{a(u)}^r \frac{2\pi r^2}{r-2\tilde{m}} \frac{1-\omega}{1+\omega} (\rho - 2Q + P_r) dr, \quad (2.34)$$

and we may rewrite the nonstatic case as

$$\beta = \int_{a(u)}^r \frac{2\pi r^2}{r-2\tilde{m}} (\tilde{\rho} + \tilde{P}) dr, \quad (2.35)$$

with

$$\tilde{P} = \frac{1}{1+\omega} [-\omega\rho - Q(1-\omega) + P_r] \quad (2.36)$$

being the effective pressure, which also reduces to the radial pressure in the static limit.

Matching the Vaidya metric to the Bondi metric at the surface ($r=a$) of the fluid distribution implies $\beta_a = \beta(u, r=a) = 0$ with the continuity of the mass function $\tilde{m}(u, r)$ (i.e., the continuity of the first fundamental form) and the continuity of the second fundamental form leads to

$$\dot{a} = - \left(1 - 2\frac{\tilde{m}_a}{a}\right) \frac{\tilde{P}_a}{\tilde{P}_a + \tilde{\rho}_a} \quad (2.37)$$

(see [31] for details).

From the coordinate transformation (2.3) the velocity of matter in Bondi coordinates can be written as

$$\frac{dr}{du} = \frac{V}{r} \frac{\omega}{1-\omega}, \quad (2.38)$$

evaluating the last expression at the surface and comparing it with (2.37) it follows that

$$\tilde{P}_a = -\omega_a \tilde{\rho}_a, \quad (2.39)$$

or equivalently using (2.33) and (2.36) we get

$$Q_a = P_{ra}, \quad (2.40)$$

which is a well-known result for radiative spheres [32].

To derive the surface equations we introduce five dimensionless functions:

$$\begin{aligned} A &\equiv \frac{a}{\tilde{m}(0)}, \\ M &\equiv \frac{\tilde{m}}{\tilde{m}(0)}, \\ u &\equiv \frac{u}{\tilde{m}(0)}, \\ F &\equiv 1 - \frac{2M}{A}, \\ \Omega &\equiv \frac{1}{1-\omega_a}, \end{aligned} \quad (2.41)$$

where $\tilde{m}(0)$ is the initial mass of the system. Using the functions just defined into (2.37) we get the first surface equation

$$\dot{A} = F(\Omega - 1). \quad (2.42)$$

This first surface equation gives the evolution of the radius of the star.

The second surface equation emerges from the luminosity evaluated at the surface of the system. The luminosity as seen by a comoving observer is defined as

$$\hat{E} = (4\pi r^2 \mathcal{Q})_{r=a}. \quad (2.43)$$

Evaluating (2.27) and (2.28) at the surface and using the expansion

$$\tilde{m}_{0a} \approx \tilde{m} - \dot{a}\tilde{m}_{1a}, \quad (2.44)$$

the luminosity perceived by an observer at rest at infinity reads

$$L = -\dot{M} = \hat{E}(2\Omega - 1)F = 4\pi A^2 \mathcal{Q}_a(2\Omega - 1)F. \quad (2.45)$$

The function F is related to the boundary redshift z_a by

$$1 + z_a = \frac{v_{\text{em}}}{v_{\text{rec}}} = F^{-1/2}. \quad (2.46)$$

Thus the luminosity as measured by a noncomoving observer located on the surface is

$$E = L(1 + z_a)^2 = -\frac{\dot{M}}{F} = \hat{E}(2\Omega - 1), \quad (2.47)$$

where the term $(2\Omega - 1)$ accounts for the boundary Doppler shift. Using relationship (2.45) together with the first surface equation we obtain the second one as

$$\dot{F} = \frac{2L + F(1 - F)(\Omega - 1)}{A}, \quad (2.48)$$

which expresses the evolution of the redshift at the surface.

The third surface equation is model dependent. For anisotropic fluids the relationship $(T_{r,\mu}^\mu)_a = 0$ can be written as

$$-\left(\frac{\tilde{P} + \tilde{\rho}}{1 - 2\tilde{m}/r}\right)_{0a} + \tilde{R}_{\perp a} - \left(\frac{2}{r}(P_r - \tilde{P})\right)_a = 0, \quad (2.49)$$

where

$$\tilde{R}_{\perp a} = \tilde{P}_{1a} + \left(\frac{\tilde{P} + \tilde{\rho}}{1 - 2\tilde{m}/r}\right)_a \left(4\pi r \tilde{P} + \frac{\tilde{m}}{r^2}\right)_a - \left(\frac{2}{r}(P_{\perp} - P_r)\right)_a. \quad (2.50)$$

It is possible to associate a physical meaning to $\tilde{R}_{\perp a}$: the first term is tied to the hydrodynamic force, the second one to the gravitational force, and the third one reflects the anisotropic character of the fluid. The latter is negative when the radial pressure is larger than the tangential pressure. In this case the fluid distribution may become more compact than in the isotropic one.

Using expansion (2.44) and

$$(\tilde{\rho} + \tilde{P})_{0a} \approx [\tilde{\rho}_a(1 - \omega_a)]_0 - \dot{a}(\tilde{P} + \tilde{\rho})_{1a},$$

where (2.39) has been used, we get

$$\frac{\dot{F}}{F} + \frac{\dot{\Omega}}{\Omega} - \frac{\tilde{\rho}_a}{\tilde{\rho}_a} + F\Omega^2 \frac{\tilde{R}_{\perp a}}{\tilde{\rho}_a} - \frac{2}{A}F\Omega \frac{P_{ra}}{\tilde{\rho}_a} = (1 - \Omega) \left[4\pi A \tilde{\rho}_a \frac{3\Omega - 1}{\Omega} - \frac{3 + F}{2A} + F\Omega \frac{\tilde{\rho}_{1a}}{\tilde{\rho}_a} + \frac{2F\Omega}{A\tilde{\rho}_a} (P_{\perp} - P_r)_a \right]. \quad (2.51)$$

Expression (2.51) generalizes the Tolman-Oppenheimer-Volkov equation to the nonstatic radiative anisotropic case.

Now we are in position to briefly summarize the HJR method [7] applied to the anisotropic case.

E. The HJR method

This method has been extensively used since last decade to obtain models of nonstatic radiating fluids from known static solutions of the Einstein equations ([6,7,33], and references therein). Its use reduces the problem of the gravitational collapse to the solution of the surface equations (2.42), (2.48), and (2.51). This procedure simplifies the resolution of the problem because these ones are a set of ordinary differential equations that can be solved by the Runge-Kutta method. The algorithm can be summarized as follows.

(1) Take a static but otherwise arbitrary interior solution of the Einstein equations for a spherically symmetric fluid distribution:

$$P_{\text{st}} = P(r), \quad \rho_{\text{st}} = \rho(r).$$

(2) The effective quantities $\tilde{\rho} \equiv \tilde{\rho}(u, r)$ and $\tilde{P} \equiv \tilde{P}(u, r)$ must coincide with ρ_{st} and P_{st} , respectively, in the static limit. We assume that the r dependence in effective quantities is the same that in its corresponding static ones. Nevertheless, in the nonstatic case the junction conditions are different, accomplishing expression (2.39). This condition allows us to find out the relation between the u dependence of $\tilde{\rho} \equiv \tilde{\rho}(u, r)$ and $\tilde{P} \equiv \tilde{P}(u, r)$.

(3) Introduce $\tilde{\rho}(u, r)$ and $\tilde{P}(u, r)$, into (2.32) and (2.35) to determine \tilde{m} and β up to three unknown functions of time.

(4) The three surface equations form a system of first-order ordinary differential equations, by solving it we find the evolution of the radius, $A(u)$, and two unknown functions of time. These ones can be related with the u dependence of $\tilde{\rho} \equiv \tilde{\rho}(u, r)$ and $\tilde{P} \equiv \tilde{P}(u, r)$.

(5) There are four unknown functions of time (A , F , Ω , and L). Thus, it is necessary to impose the evolution of one of them to solve the system of three surface equations. Usually the luminosity is taken as an input function because it can be found from observational quantities.

(6) Once these three functions are known, it is easy to find \tilde{m} and β . Therefore, the interior metric is completely defined.

(7) Now, the left-hand side of the Einstein equations (2.27)–(2.30) is known. However, the right-hand side of these equations contain five unknown quantities (ω , ρ , P_r , P_\perp , and Q). Thus, it is necessary to supply another equation to close the system of field equations. In the anisotropic static case a general equation can be found that relates the tangential pressure to the mass function, energy density and radial pressure [34]:

$$P_\perp - P_r = \frac{r}{2} P_1 + \left(\frac{\rho + P}{2} \right) \left(\frac{m + 4\pi r^3 P}{r - 2m} \right). \quad (2.52)$$

This expression is usually generalized, in the context of HJR method, to nonstatic cases by substituting for the effective variables the physical quantities [5,35]

$$P_\perp - P_r = \frac{r}{2} \tilde{P}_1 + \left(\frac{\tilde{\rho} + \tilde{P}}{2} \right) \left(\frac{\tilde{m} + 4\pi r^3 \tilde{P}}{r - 2\tilde{m}} \right). \quad (2.53)$$

Now, the Einstein equations, supplemented with (2.53), make up a close system of equations and quantities ω , ρ , P_r , P_\perp , and Q can be found.

The HJR method starts from a static interior solution of the Einstein equations [$P_{st} = P(r)$ and $\rho_{st} = \rho(r)$]. The effective variables (2.33) and (2.36) must reduce in the static case to ρ_{st} and P_{st} , respectively. Nevertheless, these quantities have a dependence on the retarded time u . We assume that the effective variables have the same r dependence as the physical variables of the static situation have. This can be justified in terms of the characteristic times for different processes involved in the collapse scenario. If the hydrostatic time scale $\mathcal{T}_{\text{hydr}}$, $\sim 1/\sqrt{G\rho}$, is much shorter than the Kelvin-Helmholtz time scale \mathcal{T}_{KH} , then in the first approximation the inertial terms in the equation of motion [$T_{r;\mu}^\mu|_{r=a} = 0$ can be ignored ([36], p. 11). The Kelvin-Helmholtz phase of the birth of a neutron star last some tens of seconds [37], whereas for a neutron star of one solar mass and a 10-km radius, we obtain $\mathcal{T}_{\text{hydr}} \sim 10^{-4}$ s. Thus, in this first approximation the r dependence of physical quantities P and ρ are the same as in the static solution. The assumption that not the physical quantities but the effective variables (2.33) and (2.36) have the same r dependence as the physical variables of the static situation is a correction to that first approximation. Therefore it is expected that the introduction of two functions of time in $\tilde{\rho}$ and \tilde{P} preserving the same r dependence as in ρ_{st} and P_{st} will yield good results. These two functions of time can be related by means of the junction condition (2.39).

If the evolution of effective variables were known the functions \tilde{m} and β could be found and the Einstein equations supplemented by (2.53) would constitute a closed system of differential equations. This method will be clarified by means of an example in Sec. IV.

III. SECOND SET OF EQUATIONS: TRANSPORT EQUATIONS

We shall use the method described above to find the heat flow, the energy density, the radial and tangential pressures,

and the velocity of the collapse. However, if one wished to explicitly find the temperature and viscous pressure, one has to resort to the transport equations laid down by EIT.

Usually classical theory [13–15] has been employed as a first approximation to the study of gravitational collapse. Nevertheless, this one presents two important disabilities [22]: (1) It predicts an infinite speed for thermal and viscous signals. (2) The equilibrium states turn out to be unstable. Therefore, as a further step in the thermodynamic study of gravitational collapse, it seems suitable to resort to a theory free of such drawbacks. As we pointed out in Sec. I the relativistic EIT may do the job. The Maxwell-Cattaneo transport equations are a particular case of those given by EIT, see for instance [23,24]. The former are decoupled expressions of the EIT transport equations and they may be understood as a first approximation to them. Thus, we consider that the dissipative flows are decoupled and the transport equations may be approximated by their Maxwell-Cattaneo form. The heat conduction equation can be written as

$$\tau_Q \dot{Q}^\nu h_\nu^\mu + Q^\mu \simeq \chi h^{\mu\nu} [T_{,\nu} - T \dot{U}_\nu], \quad (3.1)$$

where $h^{\mu\nu} = g^{\mu\nu} - U^\mu U^\nu$ is the spatial projection tensor, χ is the thermal conductivity coefficient, T the temperature and τ_Q is the relaxation time for thermal signals. The evolution of bulk viscous pressure Π is given by the expression

$$\tau_\Pi U^\alpha \Pi_{,\alpha} + \Pi \simeq -\zeta U_{;\mu}^\mu. \quad (3.2)$$

The bulk viscosity coefficient and relaxation time for bulk viscous signals are denoted by ζ and τ_Π , respectively. On the other hand, the evolution of shear viscous pressure $\pi_{\mu\nu}$ (2.24) can be written in Maxwell-Cattaneo form as

$$\tau_\pi \dot{\pi}_{\mu\nu} + \pi_{\mu\nu} \simeq 2\eta \sigma_{\mu\nu}, \quad (3.3)$$

where shear tensor $h_{(\mu}^\alpha U_{\nu); \alpha} - U_{;\alpha}^\alpha h_{\mu\nu}/3$ is denoted by $\sigma_{\mu\nu}$, τ_π corresponds to relaxation time for shear viscous signals and η indicates the shear viscosity coefficient.

Eckart transport equations are given by

$$Q^\mu \simeq \chi h^{\mu\nu} [T_{,\nu} - T \dot{U}_\nu], \quad (3.4)$$

$$\Pi \simeq -\zeta U_{;\mu}^\mu \quad (3.5)$$

and

$$\pi_{\mu\nu} \simeq 2\eta \sigma_{\mu\nu}. \quad (3.6)$$

Note that the main difference between both formulations is the presence of the relaxation time in (3.1)–(3.3). As we will show in Sec. IV this discordance is important close to the surface.

To solve this system of partial differential equations it is necessary to adopt an expression for transport coefficients χ , η , and ζ . For a mixture of matter and radiation these ones are given by (see, e.g., [8])

$$\chi = \frac{4}{3} b T^3 \tau, \quad (3.7)$$

$$\eta = \frac{4}{15} b T^4 \tau \quad (3.8)$$

and

$$\zeta = 15\eta \left[\frac{1}{3} - \left(\frac{\partial P}{\partial \rho} \right)_n \right]^2, \quad (3.9)$$

where τ denotes the mean free time of radiation (in our case neutrinos), while the constant b takes (for neutrinos) the value $7a/8$, where a is the radiation constant.

Expressions (3.1)–(3.3) imply a finite propagation speed for viscous and thermal signals. Nevertheless, to guarantee relativistic causality it is necessary to restrict the possible values of the different relaxation times. If we assume that the propagation speed of thermal and viscous signals are of the order of sound speed, then

$$\tau_Q \sim \tau_{\Pi} \sim \tau_{\pi} \sim \tau. \quad (3.10)$$

This means that the relaxation times are somewhat larger than the mean free time of radiation. Thus, if τ is known, it is possible to use (3.1) to find the temperature and, by (3.2) and (3.3) to calculate the viscous pressures.

A. Determination of τ for neutrinos

Thermal neutrino processes are important during the late stages of collapse of massive stars [9]. They help to carry thermal energy from the core to outer regions. Thus, we assume that neutrinos are principally thermally generated with energies close to $k_B T$.

A detailed study of the contribution of different processes to the neutrino transport has been given by Bruenn [10]. Our aim is to establish an approximate expression to the mean free time for neutrinos. Despite that the procedure used in this work yields good results, it is highly idealized and only approximate. A more accurate expression for τ would be desirable, but we consider that the approach below describes the process accurately enough.

At the typical densities of a neutron star, matter can capture neutrinos. The neutrino trapping helps to drive the neutrinos to local equilibrium. The matter opacity to the neutrinos takes place principally by means of electron-neutrino scattering ($e^- + \nu \rightarrow e^- + \nu$) and nucleon absorption ($\nu + n \rightarrow p + e^-$).

As a first approximation the cross section for nucleon absorption may be taken as ([9], Chap. 18)

$$\sigma_n \approx 10^{-44} \varepsilon_\nu^2 \text{ cm}^2, \quad (3.11)$$

where ε_ν is the energy of neutrinos in MeV. Then, the neutrino mean free path is given by

$$\lambda_n = \frac{1}{n_n \sigma_n} \approx \frac{10^{20}}{\rho \varepsilon_\nu} \text{ cm}, \quad (3.12)$$

where $n_n \approx 6 \times 10^{23} \rho \text{ cm}^{-3}$ [9,38] is the neutron number density.

In high energetic collisions the cross section for the electron-neutrino scattering can be approximated by [39]

$$\sigma_e \approx 10^{-44} \varepsilon_\nu \text{ cm}^2. \quad (3.13)$$

The electron number density n_e can be related to n_n by means of the electron fraction \mathcal{Y}_e ($n_e \approx n_n \mathcal{Y}_e$). Hence, the mean free path is

$$\lambda_e = \frac{1}{n_e \sigma_e} \approx \frac{10^{20}}{\rho \varepsilon_\nu \mathcal{Y}_e} \text{ cm}. \quad (3.14)$$

The effective mean free time which takes into account the neutrino zigzag path may be written as

$$\tau = \lambda \sim \sqrt{\lambda_e \lambda_n} \approx \frac{10^{20}}{\rho \sqrt{\mathcal{Y}_e \varepsilon_\nu^3}} \text{ cm}. \quad (3.15)$$

Assuming that the neutrinos are generated by thermal emission ($\varepsilon_\nu \sim k_B T$) we find the τ dependence on temperature:

$$\tau \propto T^{-3/2}. \quad (3.16)$$

A rigorous treatment of mean free time would comprise the evolution of \mathcal{Y}_e . Nevertheless, this effort does not seem advisable here due to the degree of the approximation adopted and that the range of possible values for \mathcal{Y}_e is severely restricted ($0.2 \leq \mathcal{Y}_e \leq 0.3$) [10].

It is convenient to express τ in dimensionless form to simplify the numerical treatment of Eqs. (3.1)–(3.3). In virtue of (2.41) and (3.15),

$$\tau \sim \mathcal{A} \frac{M_0}{\rho \sqrt{\mathcal{Y}_e} T^3}, \quad (3.17)$$

where the constant \mathcal{A} takes the value $10^9 \text{ K}^{3/2} \text{ m}^{-1}$, M_0 is the initial mass of star in meters, T the K temperature, and ρ the dimensionless energy density.

B. Maxwell-Cattaneo transport equations: Explicit form

The Maxwell-Cattaneo transport equations (3.1)–(3.3) can be written, by means of (3.7)–(3.9) and condition (3.10), in dimensionless form

$$\tau \dot{Q}^\nu h_\nu^\mu + Q^\mu \approx \frac{7}{6} a M_0^2 T^3 \tau h^{\mu\nu} [T_{,\nu} - T \dot{U}_\nu], \quad (3.18)$$

$$\tau U^\alpha \Pi_{,\alpha} + \Pi \approx - \frac{7}{2} a M_0^2 T^4 \tau \left[\frac{1}{3} - \left(\frac{\partial P}{\partial \rho} \right)_n \right]^2 U_{;\mu}^\mu, \quad (3.19)$$

$$\tau \dot{\pi}_{\mu\nu} + \pi_{\mu\nu} \approx \frac{7}{15} a M_0^2 T^4 \tau \sigma_{\mu\nu}, \quad (3.20)$$

where $a \approx 6.252 \times 10^{-64} \text{ cm}^{-2} \text{ K}^{-4}$.

The expression of mean free time for neutrinos (3.17) is given for a comoving observer. Thus, applying a Lorentz boost to it, it is possible to write the transport equations for an observer with radial velocity $-\omega$ respect to matter, in Bondi coordinates.

As we saw in the last section, by means of the method HJR it is possible to solve the Einstein equations. Thus, the quantities Q , ρ , P_r , P_\perp , and ω and the metric functions β and \tilde{m} are known. Resorting to expressions (3.17), (2.1),

(2.21), and (2.23) it is possible, after a straightforward calculation, to write down the Maxwell-Cattaneo equations in terms of known quantities Q , \tilde{m} , β , ω , ρ , and P_r and their derivatives.

The evolution of the heat flow (3.1) is governed by

$$f(u,r)\left(\frac{aM_0^2}{\phi}\right)^{3/5} + \frac{g(u,r)}{\mathcal{B}} \simeq \phi_0 + h(u,r)\phi_1 + w(u,r)\phi, \tag{3.21}$$

where we have introduced, for the sake of simplicity,

$$\phi = aM_0^2 T^{5/2}, \tag{3.22}$$

$$f(u,r) = \frac{15}{7} \left[\frac{Q\omega}{1-\omega^2} \left[\omega_0 + \frac{V}{r} \left(\frac{\omega}{1-\omega} \right) \omega_1 \right] + \left[Q_0 + \frac{V}{r} \left(\frac{\omega}{1-\omega} \right) Q_1 \right] \right] - \frac{15}{7} \frac{e^{2\beta} Q\omega}{1-\omega} \left[-2\beta_1 \left(1 - \frac{2\tilde{m}}{r} \right) + \frac{1}{r} \left(\tilde{m}_1 - \frac{\tilde{m}}{r} \right) + \frac{\tilde{m}_0}{V} (1-\omega) \right] + \frac{15}{7} Q\omega \frac{V}{r} \left(\frac{1+\omega}{1-\omega} \right) \dot{U}_r, \tag{3.23}$$

$$g(u,r) = \frac{15}{7} Q e^{2\beta} \sqrt{1 - \frac{2\tilde{m}}{r}} (1+\omega), \tag{3.24}$$

$$h(u,r) = - \frac{e^{2\beta}}{1-\omega} \left(1 - \frac{2\tilde{m}}{r} \right), \tag{3.25}$$

$$w(u,r) = \frac{5}{2} e^{2\beta} \left(1 - \frac{2\tilde{m}}{r} \right) \left(\frac{1+\omega}{1-\omega} \right) \dot{U}_r, \tag{3.26}$$

$$\dot{U}_r = \frac{1}{1+\omega} \left[\frac{1}{2r} - 2\beta_1 - \frac{1-2\tilde{m}_1}{2(r-2\tilde{m})} \right] + r e^{-2\beta} \left(\frac{1-\omega}{1+\omega} \right) \frac{\tilde{m}_0}{(r-2\tilde{m})^2} - \frac{1}{(1+\omega)^2(1-\omega)} \left[\omega\omega_1 + r e^{-2\beta} \frac{1-\omega}{r-2\tilde{m}} \omega_0 \right], \tag{3.27}$$

and

$$\mathcal{B} = \mathcal{A} \frac{M_0}{\rho \sqrt{\mathcal{Y}_e}}. \tag{3.28}$$

The bulk viscous pressure (3.2) can be found by solving the partial differential equation

$$-\frac{7}{2} aM_0^2 T^4 e^{2\beta} \sqrt{1 - \frac{2\tilde{m}}{r}} \sqrt{\frac{1+\omega}{1-\omega}} \left[\frac{1}{3} - \left(\frac{\partial P}{\partial \rho} \right)_n \right]^2 \theta \simeq \Pi_0 + \left[e^{2\beta} \left(1 - \frac{2\tilde{m}}{r} \right) \frac{\omega}{1-\omega} \right] \Pi_1 + \left[e^{2\beta} \sqrt{1 - \frac{2\tilde{m}}{r}} (1+\omega) \frac{T^{3/2}}{\mathcal{B}} \right] \Pi. \tag{3.29}$$

where the expansion θ can be written as

$$\theta = U_{;\mu}^\mu = \sqrt{1 - \frac{2\tilde{m}}{r}} \frac{2\omega}{\sqrt{1-\omega^2}} \left(\frac{1}{r} + \beta_1 \right) + \frac{1}{\sqrt{1-2\tilde{m}/r}} \frac{\omega}{\sqrt{1-\omega^2}} \left(\frac{\tilde{m}}{r^2} - \frac{\tilde{m}_1}{r} \right) + e^{-2\beta} \frac{\tilde{m}_0}{r(1-2\tilde{m}/r)^{3/2}} \sqrt{\frac{1-\omega}{1+\omega}} + \frac{\sqrt{1-2\tilde{m}/r}}{\sqrt{1-\omega^2}(1+\omega)} \left[\frac{\omega_1}{1-\omega} - e^{-2\beta} \frac{\omega_0}{1-2\tilde{m}/r} \right]. \tag{3.30}$$

The description of shear viscous pressure evolution (3.3) is given, as in the other two dissipative flows, by a first-order partial differential equation

$$-\frac{14M_0^2}{15\sqrt{3}} aT^4 e^{2\beta} \sqrt{1 - \frac{2\tilde{m}}{r}} \sqrt{\frac{1+\omega}{1-\omega}} \sigma \simeq \pi_0 + \left[e^{2\beta} \left(1 - \frac{2\tilde{m}}{r} \right) \frac{\omega}{1-\omega} \right] \pi_1 + \left[e^{2\beta} \sqrt{1 - \frac{2\tilde{m}}{r}} (1+\omega) \frac{T^{3/2}}{\mathcal{B}} \right] \pi, \tag{3.31}$$

where $\sigma^2 = (1/2)\sigma_{\mu\nu}\sigma^{\mu\nu}$ and

$$\sigma = \frac{\sqrt{3}}{r} \left[-\frac{\omega}{\sqrt{r}} \sqrt{\frac{r-2\tilde{m}}{1-\omega^2}} + \frac{\theta}{3} r \right]. \quad (3.32)$$

The transport coefficients (3.7)–(3.9) as measured by a comoving observer read

$$\chi = \frac{4}{3} b c^2 T^{3/2} \frac{Y}{\rho \sqrt{\mathcal{Y}_e}}, \quad (3.33)$$

$$\eta = \frac{4}{15} b T^{5/2} \frac{Y}{\rho \sqrt{\mathcal{Y}_e}}, \quad (3.34)$$

$$\zeta = 4bT^{5/2} \left[\frac{1}{3} - \left(\frac{\partial P}{\partial \rho} \right) \right]^{2r} \left[\frac{Y}{\rho \sqrt{\mathcal{Y}_e}} \right], \quad (3.35)$$

with $Y \approx 4.173 \times 10^{24} \text{ g cm}^{-3} \text{ K}^{3/2} \text{ s}$.

The system of three partial differential equations (3.21), (3.29), and (3.31) can be solved provided initials, finals, and boundary conditions are given. The boundary condition for temperature in the heat conduction equation (3.21) deserves special attention. As shown in Sec. IV C, the boundary condition for the temperature must satisfy some requirements. After solving the heat conduction equation, we shall find the temperature, and using it in the evolution equations (3.29), and (3.31) the bulk and shear viscous pressure will be determined. Once the temperature is known, it will be easy to find the coefficients of heat conductivity, shear viscosity and bulk viscosity, from Eqs. (3.33)–(3.35), respectively.

IV. APPLICATION TO THE GOKHROO-MEHRA CONFIGURATION

As we have seen in Sec. III, the HJR method starts from a static solution of Einstein's equations. It is possible to find numerical models based in nuclear physics as solutions of the Einstein equations. However, the uncertainties introduced by this procedure in the HJR method make it desirable to start from a static analytical model instead. On the other hand, it is suitable to adopt an initially static fluid distribution not excessively idealized. Some analytic anisotropic static solutions of the field equations are known [1,2,40–44]. We shall adopt the static form of Gokhroo and Mehra (GM) [25] to illustrate the application of method described above. This solution corresponds to a fluid with variable energy density in which some anisotropy is initially present even in absence of radiation. It leads, under some circumstances, to densities and pressures similar to the Bethe-Börner-Sato (BBS) *Newtonian* state equation [9,11,36,45]. Thus, this solution presents a compromise between the realism of the solutions based in nuclear physics and the desirable analytic expression of the static solution.

A. Introduction of the GM configuration in the HJR method

Following the first point of the HJR method (Sec. II E), it is necessary to start from a static solution (ρ_{st} and P_{st}) of the

Einstein equations. In the static solution of Gokhroo and Mehra [25] the energy density and radial pressure are assumed to be

$$\rho(r) = \rho_c \left(1 - k \frac{r^2}{a^2} \right) \quad (4.1)$$

and

$$P_r(r) = P_c \left(1 - \frac{2m}{r} \right) \left(1 - \frac{r^2}{a^2} \right)^n, \quad (4.2)$$

where $0 \leq k \leq 1$ and $n \geq 1$ are constants. The central energy density and radial pressure are denoted by ρ_c and P_c , respectively, and in the static case they are related by means of a constant λ through the expression

$$P_c = \lambda \rho_c. \quad (4.3)$$

Thus, we identify ρ_{st} as $\rho(r)$ and P_{st} as $P_r(r)$. The tangential pressure is

$$\begin{aligned} P_{\perp}(r) - P_r(r) &= \frac{r}{2} [P_r]_1 + \left(\frac{\rho + P_r}{2} \right) \left(\frac{m(r) + 4\pi r^3 P_r}{r - 2m(r)} \right) \\ &= \frac{3}{10} \frac{k P_c}{a^2} \alpha r^4 \left(1 - \frac{r^2}{a^2} \right)^n + \frac{r^2}{2(1 - 2m/r)} \Phi, \end{aligned} \quad (4.4)$$

where

$$\begin{aligned} \Phi &= 2P_c \left(1 - 2\frac{m}{r} \right)^{2r} \left[2\pi P_c \left(1 - \frac{r^2}{a^2} \right)^{2n} \right. \\ &\quad \left. - \frac{n}{a^2} \left(1 - \frac{r^2}{a^2} \right)^{n-1} \right] \\ &\quad + \frac{\alpha \rho_c}{2} \left(1 - \frac{3k}{5} \frac{r^2}{a^2} \right) \left(1 - k \frac{r^2}{a^2} \right), \end{aligned} \quad (4.5)$$

with

$$\alpha = \frac{8\pi\rho_c}{3}. \quad (4.6)$$

In applying the HJR method (second point of the algorithm) we assume that the effective variables $\tilde{\rho}(u, r)$ and $\tilde{P}(u, r)$ have the same r dependence as the physical quantities $\rho(r)$ and $P(r)$. The time dependence of these is introduced by two arbitrary functions of time $K(u)$ and $G(u)$. The form proposed here is

$$\tilde{\rho} = \tilde{\rho}_c(u) \left(1 - K(u) \frac{r^2}{a^2} \right), \quad (4.7)$$

and

$$\tilde{P} = \tilde{P}_c(u) \left(1 - 2\frac{\tilde{m}}{r} \right) \left(1 - G(u) \frac{r^2}{a^2} \right)^n, \quad (4.8)$$

where

$$\tilde{\rho}_c(u) = \rho_c \frac{K(u)}{K(0)} \equiv \rho_c \frac{K}{K_0}, \tag{4.9}$$

$$\tilde{P}_c(u) = P_c \frac{K(u)}{K(0)} \equiv P_c \frac{K}{K_0}. \tag{4.10}$$

The central energy density and radial pressure in the final equilibrium state must differ from their values in the initial static case. Thus, we introduce their *effective* variables $\tilde{\rho}_c$ and \tilde{P}_c . These variables do not enjoy any physical meaning during the collapse, but they coincide with the central energy density and radial pressure in the static case. Because of this, it is necessary to introduce a time dependence in $\tilde{\rho}_c$ and \tilde{P}_c . The correctness of expressions (4.7) and (4.8) may be seen *a posteriori* at the sight of the obtained results, Sec. V below. As mentioned in Sec. II E, the junction condition (2.39) allows us to relate both unknown functions of time K and G . Using (4.7) and (4.8) in (2.39) and by means of (2.41) they are related by the expression

$$(1 - G)^n = \frac{(1 - \Omega)(1 - K)}{F\Omega\lambda}. \tag{4.11}$$

To find an expression for $\tilde{m}(u, r)$ and $\beta(u, r)$ (third point) we resort to expressions (2.32) and (2.35). In virtue of (4.7) the mass function can be written as

$$\tilde{m} = \int_0^r 4\pi r^2 \tilde{\rho} dr = \frac{\tilde{\alpha} r^3}{2} \left(1 - \frac{3K}{5} \frac{r^2}{A^2} \right), \tag{4.12}$$

where

$$\tilde{\alpha} = \frac{8\pi\tilde{\rho}_c}{3} = \alpha \frac{K}{K_0} \tag{4.13}$$

and the radius of the star a is written from (2.41) as A because, without loss of generality, the initial mass is taken as unity. The expression of $\beta(u, r)$, by means of (4.7) and (4.8), reads

$$\beta = \frac{3\lambda\tilde{\alpha}A^2}{8G(n+1)} \left[(1-G)^{n+1} - \left(1 - G \frac{r^2}{A^2} \right)^{n+1} \right] - \frac{5}{16} \ln \left[\frac{1 - \tilde{\alpha}r^2 + (3K\tilde{\alpha}/5A^2)r^4}{1 - \tilde{\alpha}A^2 + (3K\tilde{\alpha}/5)A^2} \right] + \frac{\tilde{\alpha}}{16} \mathcal{I}, \tag{4.14}$$

where \mathcal{I} may take different values depending on the relation between $\tilde{\alpha}$ and K/A^2 :

For $12K/5A^2 > \tilde{\alpha}$, \mathcal{I} takes the form

$$\mathcal{I} = \frac{2}{\xi} \left[\arctan \left(\frac{\tilde{\alpha}(6Kr^2 - 5A^2)}{5A^2\xi} \right) - \arctan \left(\frac{\tilde{\alpha}(6K - 5)}{5\xi} \right) \right], \tag{4.15}$$

where

$$\xi \equiv \sqrt{\frac{12\tilde{\alpha}K}{5A^2} - \tilde{\alpha}^2}. \tag{4.16}$$

For $\tilde{\alpha} > 12K/5A^2$,

$$\mathcal{I} = \frac{1}{\xi} \ln \left[\left(\frac{\tilde{\alpha}(6Kr^2 - 5A^2) - 5A^2\xi}{\tilde{\alpha}(6Kr^2 - 5A^2) + 5A^2\xi} \right) \left(\frac{\tilde{\alpha}(6K - 5) + 5\xi}{\tilde{\alpha}(6K - 5) - 5\xi} \right) \right], \tag{4.17}$$

and

$$\xi \equiv \sqrt{\tilde{\alpha}^2 - \frac{12\tilde{\alpha}K}{5A^2}}. \tag{4.18}$$

For $\tilde{\alpha} = 12K/5A^2$, \mathcal{I} takes a more simple form

$$\mathcal{I} = -\frac{16}{\tilde{\alpha}^3} \left[\frac{1}{\tilde{\alpha}r^2 - 2} - \frac{1}{\tilde{\alpha}A^2 - 2} \right]. \tag{4.19}$$

Following the fourth point of the HJR method it is necessary to relate the unknown functions of time K and G with the functions A , Ω , F , or L . To this end, we evaluate expression (4.12) in the surface of the star,

$$M = \tilde{m}_a = \frac{K}{K_0} \left(\frac{\alpha A^3}{2} \right) \left(1 - \frac{3K}{5} \right). \tag{4.20}$$

On the other hand, in virtue of (2.41) the total mass of the system is

$$M = \frac{A}{2} (1 - F). \tag{4.21}$$

Equating the two last expressions it is possible to find the dependence of K on A and F ,

$$K(u) = K(A, F) = \frac{5}{6} \left[1 \pm \sqrt{1 - \left(\frac{12K_0}{5\alpha} \right) \left(\frac{1-F}{A^2} \right)} \right]. \tag{4.22}$$

The dependence of G on time (or equivalently on A , F , and Ω) can be established by substituting the last expression in (4.11). Thus, introducing the expressions $K(A, F)$ and $G(A, F, \Omega)$ in (4.7), (4.8), (4.12), and (4.14), $\tilde{\rho}$, \tilde{P} , \tilde{m} , and β are known throughout the star and for all times as functions of r and A , F , and Ω .

To ascertain the physically meaningful sign in (4.22), we evaluate it at the initial time,

$$\frac{6}{5} K_0 - 1 = \pm \sqrt{1 - \frac{24K_0}{5\alpha A^3}}, \tag{4.23}$$

where we have made use of (2.41) with $\tilde{m}(0) = 1$. Therefore, if the initial value of the function K exceeds $5/6$ we must adopt the positive sign in (4.22), and the negative one otherwise.

The functions A , F , and Ω can be found from the system of surface equations if the luminosity is known (point five of the method). The first two surface equations (2.42) and (2.48), are model independent. In order to find a valid expression for the third one we resort to the expression given in the last point of the algorithm (2.53) which in virtue of (4.7), (4.8), and (4.12) can be written as

$$P_{\perp}(u,r) - P_r(u,r) = \frac{3}{10} \frac{k\tilde{P}_c}{a^2} \tilde{\alpha} r^4 \left(1 - G \frac{r^2}{a^2}\right)^n + \frac{r^2}{2(1-2\tilde{m}/r)} \tilde{\Phi}, \quad (4.24)$$

where

$$\tilde{\Phi} = 2\tilde{P}_c \left(1 - 2\frac{\tilde{m}}{r}\right)^2 \left[2\pi\tilde{P}_c \left(1 - G \frac{r^2}{a^2}\right)^{2n} - \frac{nG}{a^2} \left(1 - G \frac{r^2}{a^2}\right)^{n-1} \right] + \frac{\tilde{\alpha}\tilde{\rho}_c}{2} \left(1 - \frac{3K}{5} \frac{r^2}{a^2}\right) \left(1 - K \frac{r^2}{a^2}\right). \quad (4.25)$$

Therefore, the system of surface equations is

$$\dot{A} = F(\Omega - 1), \quad (4.26)$$

$$\dot{F} = \frac{1}{A} [2L + F(1-F)(\Omega - 1)], \quad (4.27)$$

and

$$\dot{\Omega} = -\frac{\dot{F}}{F} \Omega + \frac{\dot{K}}{K} \frac{1-2K}{1-K} \Omega + \frac{4L\Omega^2}{3\tilde{\alpha}A^3(2\Omega-1)(1-K)} + \Omega(1-\Omega)\xi, \quad (4.28)$$

where

$$\xi = \frac{3\tilde{\alpha}}{2} A(1-K) \left(\frac{3\Omega-1}{\Omega}\right) - \frac{3+F}{2A} + \frac{2F\Omega}{A(1-K)} (\Psi - K), \quad (4.29)$$

$$\Psi = \frac{3}{10} \lambda \tilde{\alpha} A^2 K (1-G)^n + \frac{A^2}{2F} \left[\frac{3\tilde{\alpha}}{2} \lambda^2 F^2 (1-G)^{2n} - \frac{2n\lambda G}{A^2} F^2 (1-G)^{n-1} + \frac{\tilde{\alpha}}{2} \left(1 - \frac{3K}{5}\right) (1-K) \right]. \quad (4.30)$$

This system of differential equations can be solved for a given set of initial values of A , F , and Ω imposing a boundary condition (in this case the luminosity L).

The initial central energy density can be written, by means of (4.6) and (4.23), as a function of initial radius and K_0 :

$$\rho_c = \frac{15}{4\pi A_0^3 (5-3K_0)}. \quad (4.31)$$

Thus, a large radius implies a low central energy density. Moreover, the positive character of the discriminant in (4.22) implies some restrictions about the evolution of the total mass M of the star. During the collapse it must satisfy the inequality

$$M \leq \frac{5\alpha}{24K_0} A^3. \quad (4.32)$$

In the static case a non-negative value of K (i.e., K_0), ensures the condition $d\rho/dr \leq 0$, while condition $K_0 \leq 1$ leads to a positive energy density. The effective energy density lacks of physical meaning when the star is collapsing. Therefore, the last argument cannot be applied to decide the range of values of function K here. Evaluating (2.33) in the surface and using (2.40) and (2.41) we obtain

$$\tilde{\rho}_a = \frac{\Omega}{2\Omega-1} (\rho_a - P_{ra}). \quad (4.33)$$

Ω lies in the range $1/2 < \Omega < \infty$, further the condition $\rho \geq P_r$ must be satisfied. Thus, from the last expression, $\tilde{\rho}_a \geq 0$. Applying this restriction to (4.7) evaluated in the surface we obtain

$$K(1-K) \geq 0 \Rightarrow 0 \leq K \leq 1, \quad (4.34)$$

therefore the range of values physically admissible for K coincides with the static one.

A last remark is in order before numerically solving the system of surface equations. Note that the generalization adopted for the tangential pressure (2.53) does not allow explosive models [35].

B. Evolution of the GM configuration

We now are prepared to study the evolution of the initial static fluid distribution described above in a particular case. To this end, it is necessary to adopt a specific initial configuration. The neutrinos can be studied in the diffusive regime if the density is higher than $10^{11} \sim 10^{12} \text{ g cm}^{-3}$. As mentioned in the Introduction, the neutrino trapping is an important source of viscosity. Because of that, in our diffusive model, the energy density in the surface must be, at least, about $10^{12} \text{ g cm}^{-3}$. On the other hand a neutron star with a radius of about 10 km, has a central density not far from $10^{15} \text{ g cm}^{-3}$ [9,11]. In this diffusive model, the energy density in the center is a thousand times the corresponding to the surface. Thus, from (4.1), $K_0 = 0.999$. From expression (4.31) one can find the initial radius for a given initial stellar mass. Introducing the usual dimensions in (4.31) we obtain

$$\rho_c = \frac{c^2}{G} \frac{15}{4\pi A_0^3 (5-3K_0) M_0^2}, \quad (4.35)$$

where the initial mass M_0 is given in geometrized units. Assuming $A_0 = 6$, the initial mass is close to $1.3 M_{\odot}$. The corresponding initial radius can be found from (2.41):

$$a_0 = A_0 M_0 \approx 11\,521 \text{ m}. \quad (4.36)$$

These values for the initial radius and mass are in the range of the usually accepted as typical for neutron stars. So we specifically adopt as an initial configuration

$$\rho_c \approx 1.01 \times 10^{15} \text{ g cm}^{-3},$$

$$\rho_a \approx 1.01 \times 10^{12} \text{ g cm}^{-3},$$

$$M_0 = 1.3 M_{\odot}$$

and

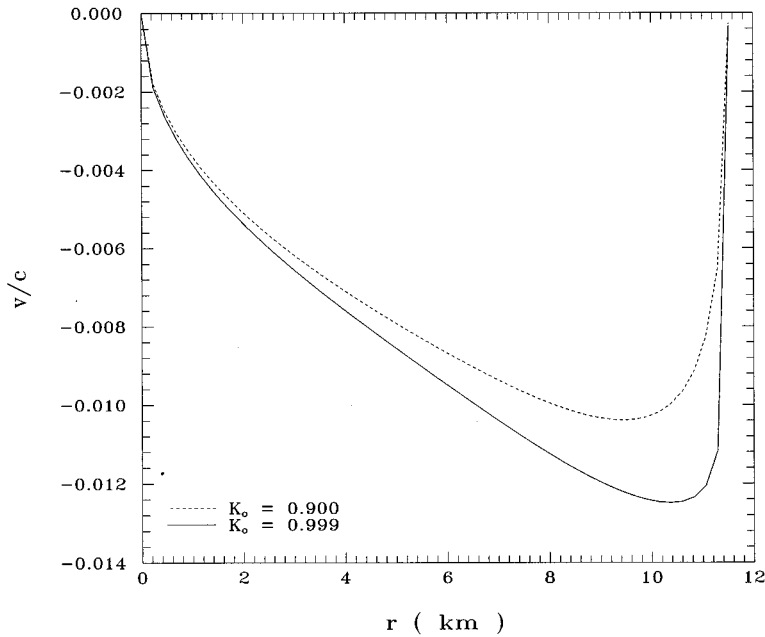


FIG. 1. Velocity profile a for given constant Schwarzschild time ($T=0.9$ ms) and two different values of K_0 . All the figures made at constant Schwarzschild time were constructed from expression (2.7).

$$a_0 \approx 11\,521 \text{ m}, \quad (4.37)$$

corresponding to a dense neutron star in which the diffusion approximation for neutrinos holds.

To completely determine the initial conditions it is necessary to give a relationship between the energy density and pressure in the center of the star (4.3). Also the parameter n occurring in the expression for pressure in the static case (4.2) must be imposed. If we assume the center of the star as a highly relativistic Fermi gas, then $\lambda = 1/3$. In addition we take $n = 1$ for simplicity.

Therefore, the initial conditions for the system of surface equations (4.26)–(4.28) are

$$\begin{aligned} A_0 &= 6, \\ F_0 &= \frac{2}{3}, \\ \Omega_0 &= 1, \\ K_0 &= 0.999, \\ P_c &= \frac{1}{3} \rho_c, \end{aligned} \quad (4.38)$$

and

$$n = 1.$$

These ones correspond to a neutron star, initially at rest, with a redshift ($z_a = 1/\sqrt{F} - 1$) close to 0.22.

The boundary condition, necessary to solve the system of surface equations, is supplied by the luminosity. We assume a Gaussian pulse for L centered in $u = u_{\text{peak}}$, and width Λ :

$$L = -\dot{M} = \frac{M_r}{\Lambda \sqrt{2\pi}} \exp\left(-\frac{1}{2} \left[\frac{u - u_{\text{peak}}}{\Lambda}\right]^2\right). \quad (4.39)$$

Note that M_r is the total energy radiated by the star in the collapse. The values adopted for M_r , Λ , and u_{peak} are $0.01M_0$, 15, and 150, respectively. We have imposed the energy conditions for imperfect fluids [46] and the restriction $-1 < \omega < 1$.

It is worth emphasizing the behavior of this model close to surface of the star. The surface collapses more slowly than the adjacent layers (Fig. 1). It may be traced to the profile of the pressure gradient in this region. As seen in Fig. 2, its absolute value is larger in the surface than in the adjacent layers, which find a lesser resistance to collapse. Similar behavior is observed for lower values of K_0 . Nevertheless, for low K_0 the variation in the pressure gradient is smaller than for large K_0 and, consequently, the difference between the velocity of surface and adjacent layers is not too high.

The value of K_0 largely determines the radius of the star once the collapse is finished. The higher K_0 , the lower final radius. This behavior can be related to the fact that values of K_0 far from unity follows from an equation of state close to incompressibility. Thus, in these cases, the velocity of the surface is not very high and possible variations in the radius are restricted. The highest variations in energy density and radial pressure take place in the most external layers, which comprise approximately 1000 m below the surface (Figs. 3 and 4).

The evolution of the energy density in the surface is depicted in Fig. 5. For $K_0 = 0.9$ [$\rho_a(u=0) \approx 8.78 \times 10^{13} \text{ g cm}^{-3}$] it varies about 6.5%, while for $K_0 = 0.999$ the final energy density in the surface gets nine times its initial value. This behavior, with that of the velocity, hints that the compression of the star is higher in the shells near the surface. This is likely due to the radiation generated in the collapse. As it is shown in Fig. 6 the heat flow is more intense in the inner shells than in the more external ones.

Initially the viscous pressure vanishes due to the absence of radiation. This condition is also fulfilled in the equilibrium situation once the collapse is over. Its contribution to the

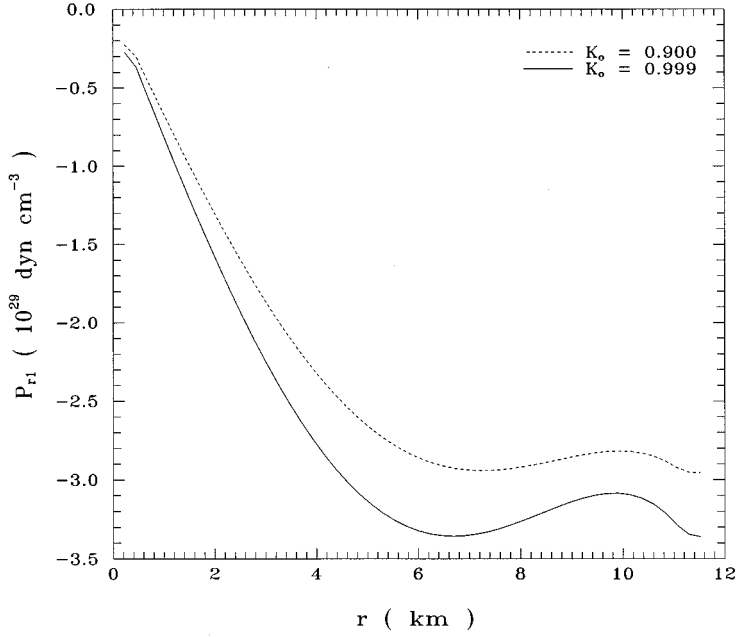


FIG. 2. Pressure gradient profile. The decrease of $|P_{r1}|$ close to the surface is, probably, the cause of the behavior shown by the velocity in this region. Schwarzschild time $T=0.9$ ms.

tangential pressure during the collapse must be established by means of the transport equations.

C. Boundary and initial conditions for the transport equations

We have solved the transport equation for the heat flow (3.21) for different boundary conditions. The interior solution found for the temperature ceases to be sensitive to the boundary condition about 500–700 m below the surface. This hints that the energy of the emergent neutrinos is not correlated with its energy beyond this external region and, consequently, most of the neutrinos escaping the star have been generated in the inner limit of this region. This agrees with the idea of the neutrinosphere [38]. A possible cause of this behavior can be found in the abrupt decrease of the heat

flow close to surface, that follows from the similar behavior shown by the energy density and radial pressure in this zone. As the model of Gokhroo and Mehra, the BBS model and others based on nuclear physics show the same features [9,11]. Thus, the neutrinosphere seems to occur whenever the adopted model is not highly idealized.

Aimed to establish the boundary condition for the temperature we introduce the effective temperature, T_{eff} . This one is usually defined by means of

$$E = [4\pi r^2 \sigma T_{\text{eff}}^4]_{r=a}, \quad (4.40)$$

where $\sigma = bc/4$, and

$$E = [4\pi r^2 \varepsilon]_{r=a} \quad (4.41)$$

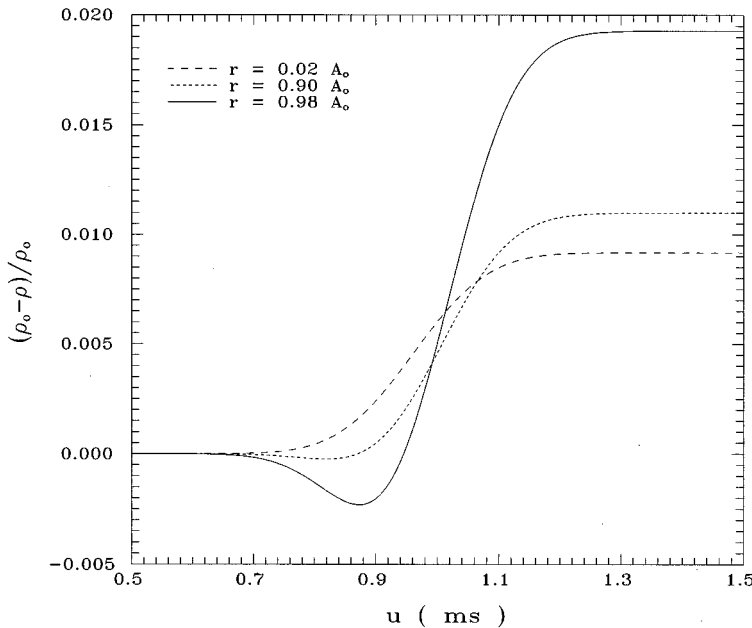


FIG. 3. Relative variation of the energy density as a function of the retarded time u . The corresponding value for K_0 is 0.999. ρ_0 denotes the initial energy density.

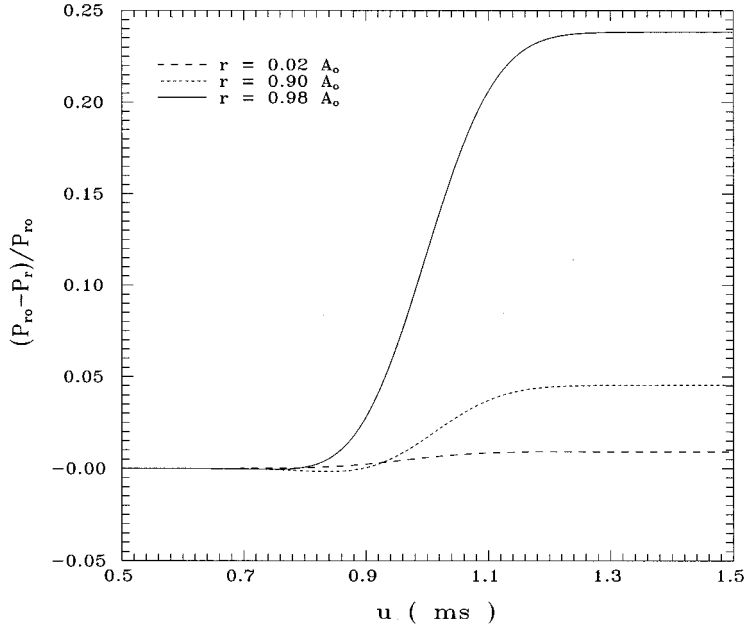


FIG. 4. Relative variation of the radial pressure as a function of the retarded time u . $K_0=0.999$.

is the luminosity as measured by the noncomoving observer momentarily located on the surface. It is to say T_{eff} would be the temperature in the surface of the star if it would radiate as a black body. The idea of effective temperature, see for instance ([9], p. 586) and ([38], p. 295), is applicable to the most external layers of the star. It is related with the material temperature by the expression

$$T^4 = \frac{1}{2} T_{\text{eff}}^4 \left(1 + \frac{3}{2} \tau \right), \tag{4.42}$$

where τ is the optical depth (i.e., $d\tau = -dr/\lambda_{\text{eff}}$).

According to last expression, if $\tau = 2/3$ the effective temperature coincides with the material one. Thus, most of the emergent neutrinos are generated in a shell close to $\tau \sim 2/3$.

This one is, in the model under consideration, about 500 m below the surface. At the surface τ vanishes. Hence, the material temperature of the surface can be written as

$$[T^4]_a = \frac{1}{2} [T_{\text{eff}}^4]_a. \tag{4.43}$$

The boundary condition can be found from the last expression together with (2.43), (2.47), (4.40), and (4.43). It reads

$$T_a^4 = Q_a \frac{2\Omega - 1}{2\sigma}. \tag{4.44}$$

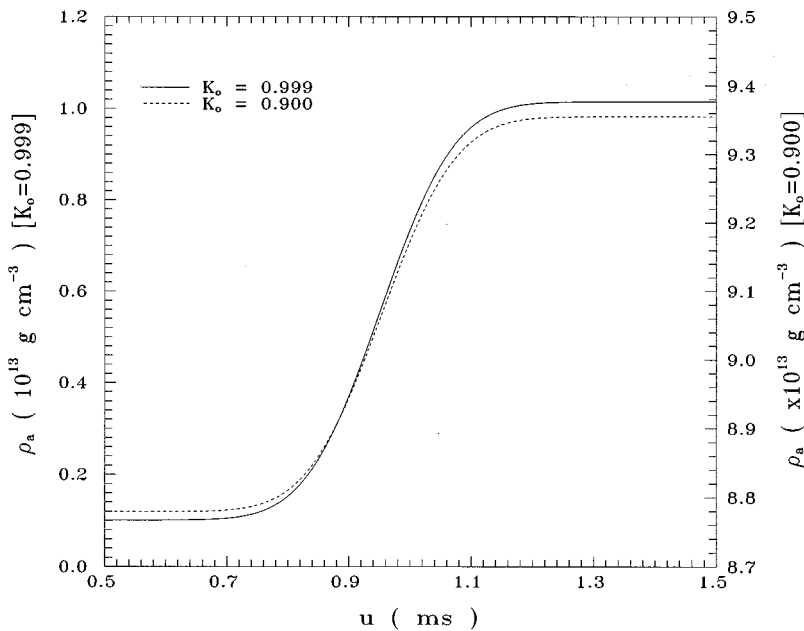


FIG. 5. Energy density evolution at the surface for two different models ($K_0=0.999$ and $K_0=0.9$). Note the different scale used in each case.

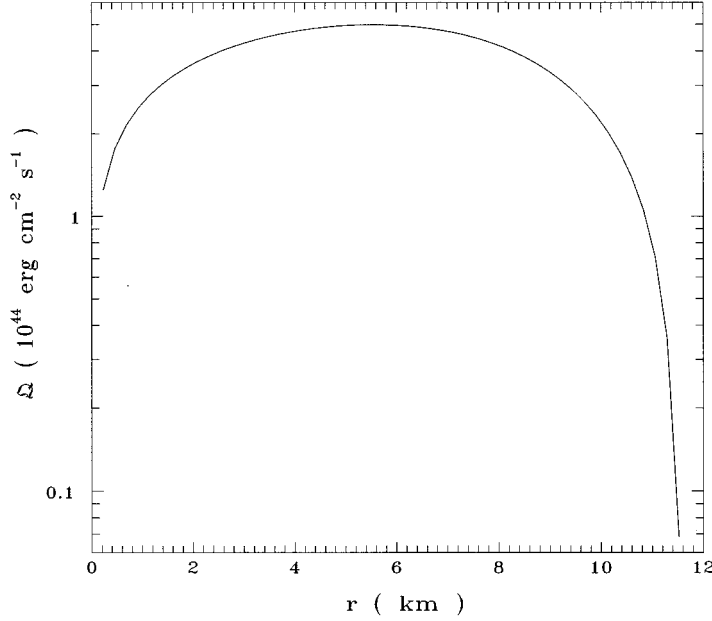


FIG. 6. Radial heat flow \mathcal{Q} as measured by the Minkowskian observer locally comoving with matter. $K_0=0.999$ and $T=0.95$ ms.

This condition on the surface affects the evolution of the temperature in the layers close to the surface but not the evolution of the inner temperature (Fig. 7).

To find explicitly the bulk and shear viscous pressure it is necessary to impose initial and boundary conditions. Something about the initial condition for the viscous pressure has been noted at the end of the last subsection. We assume that viscous processes appear because of the interaction between matter and neutrinos. Therefore, initially Π and π must vanish because of the absence of radiation.

At the center of the star the isotropy condition ($P_\perp = P_r$) is fulfilled. Thus, in virtue of (2.19) the relation

$$\lim_{r \rightarrow 0} \left(\nu - \frac{3}{2} \pi \right) = 0 \quad (4.45)$$

must be satisfied. And as a consequence of the regularity condition $[\tilde{m}]_{r=0} = 0$, at the center of the star the generation of neutrinos is forbidden. Therefore we assume that both viscous pressures, vanish at $r=0$. Thus, the boundary conditions imposed on (3.29) and (3.31) are

$$[\Pi]_{r=0} = [\pi]_{r=0} = 0 \nabla u, \quad (4.46)$$

and, from (4.45),

$$[\nu]_{r=0} = 0 \nabla u. \quad (4.47)$$

D. Temperature and viscous pressure: main results

We have used the Maxwell-Cattaneo transport equations instead of Eckart's since the latter ones violate relativistic

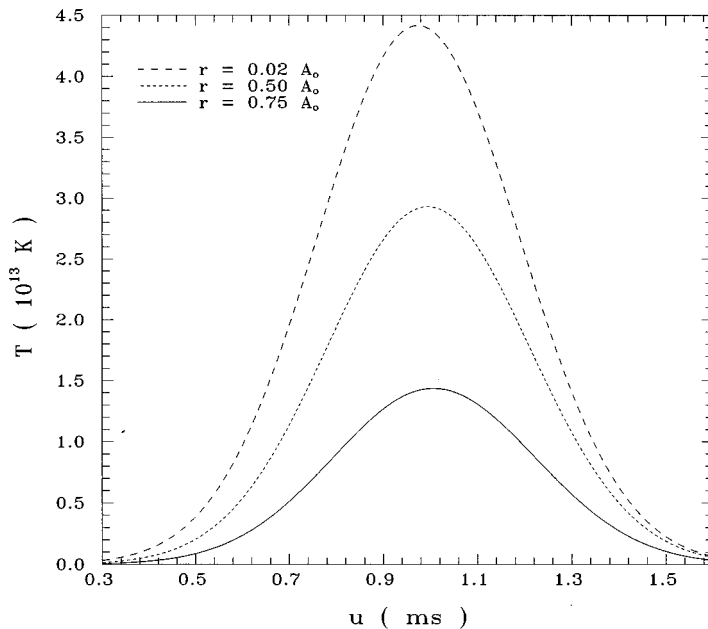


FIG. 7. Temperature as measured by an observed momentarily located at the surface. Its maximum value at the surface is about 5.44×10^{11} K. Here, and in the following figures, $\mathcal{V}_e = 0.2$.

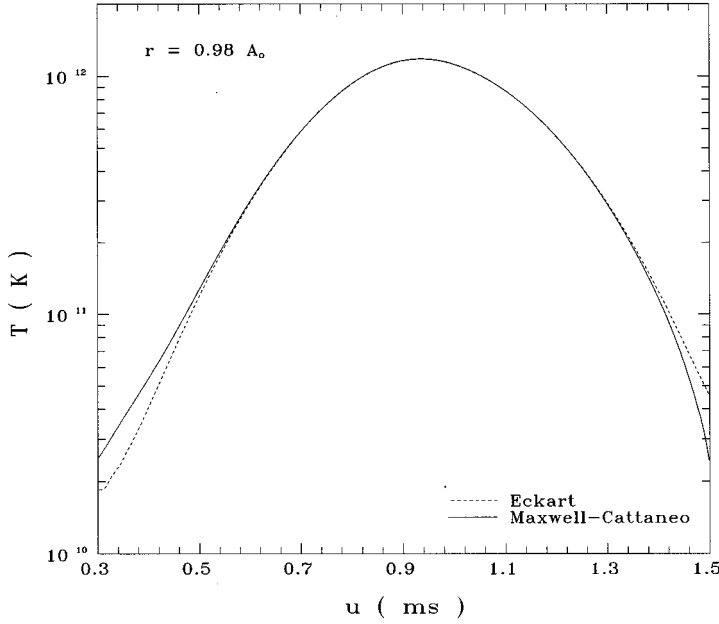


FIG. 8. Difference in the neutrinosphere between the temperature found by means of the Eckart and Maxwell-Cattaneo transport equations.

causality. The temperature in the inner layers found by means of (3.21) is the same as the one obtained using (3.4) (i.e., Fourier's law). Nevertheless, in the neutrinosphere the differences between both solutions cannot be neglected, especially in the first and late stages of the collapse (Fig. 8). The main difference between Maxwell-Cattaneo and Eckart heat transport equations is the presence of the term $\tau \dot{Q}^\nu h_\nu^\mu$, which introduces in (3.21) the term

$$f(u, r) \left(\frac{aM_0^2}{\phi} \right)^{3/5}, \quad (4.48)$$

while Q^μ leads to

$$\frac{g(u, r)}{\mathcal{B}}. \quad (4.49)$$

In the neutrinosphere and in the case under consideration one has $f(u, r) \sim 0.1 g(u, r)$ and $\mathcal{B} \sim 10^{18}$; i.e., both terms are of about the same order when temperature approaches 10^{11} K. Thus, the effects introduced by the presence of a relaxation term in heat transport equation are important there.

The high value reached by the temperature (Fig. 7) validates the adopted initial and final conditions: the approximation that in the static case the temperature for the neutron star vanishes. Applying this condition with (4.44) to expression (3.21) allows us to find the evolution of the temperature. Once the temperature is known, the transport coefficients can be calculated with the help of (3.33)–(3.35).

The bulk viscous coefficient, ζ , vanishes at the center of the star because of the state equation (4.38) adopted there. In the shells close to the center the state equation is near to $P_r = \rho/3$. Thus, the value of ζ is less than corresponding to shear viscous coefficient (η) (Figs. 9 and 10). Nevertheless, in virtue of (3.9), in stars with a central equation of state different from the adopted in this case, i.e., not highly relativistic, ζ can be of the order of η . On the other hand a

comparison among the terms in the evolution equations (3.29) and (3.31) points out that the term

$$\left[\frac{1}{3} - \left(\frac{\partial P}{\partial \rho} \right)_n \right]^2 \quad (4.50)$$

is responsible for the main differences between the bulk and shear viscous pressures.

In the region in which the energy density is roughly 10^{14} g cm $^{-3}$ we find for the shear viscosity coefficient values about 10^{28} dyn cm $^{-2}$ s $^{-1}$, which is 10^9 times higher than the corresponding to the interactions among electrons, protons and neutrons at the same density [47]. This underlines the importance of the neutrino trapping as a source of viscosity in the stellar collapse. Similarly the thermal conductivity coefficient is greater for neutrino scattering than that mentioned [47,48].

The evolution of π is shown in Fig. 11 for different layers of the star. The shear viscosity value rises swiftly from zero, at the center of the star, and becomes an important source of anisotropy in the core of the star (Fig. 12). For distances from the center larger than 2 km, π can be neglected as compared with ρ as a source of anisotropy.

The bulk viscous pressure is depicted in Fig. 13. In this model Π can be neglected against π in the innermost shells. However, in the peripheral layers Π and π , are of the same order.

V. DISCUSSION

In this paper we have used the HJR method to generate nonstatic solution departing from the static anisotropic fluid distribution of Gokhroo and Mehra [25]. This model shows an initial nonuniform energy density. The presence in the expression for the energy density of the parameter K allows us to model without difficulties the initial features of the star

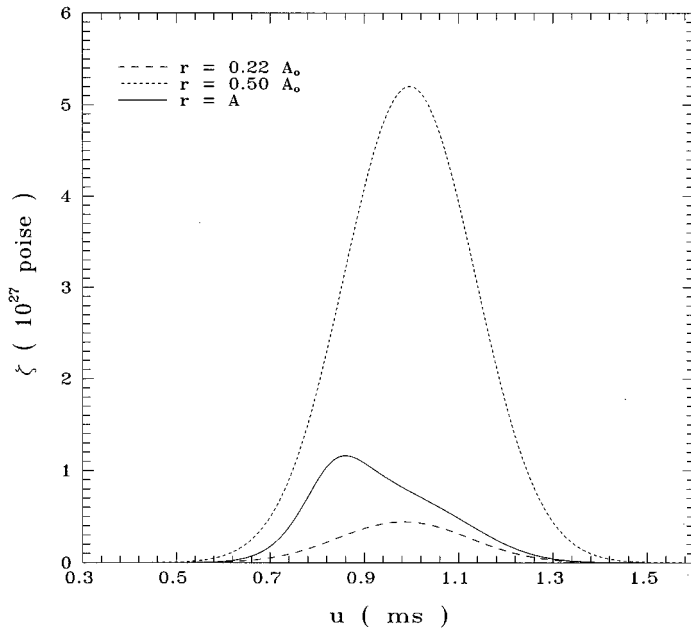


FIG. 9. Evolution of the bulk viscosity coefficient ζ .

according to the radiation limit adopted on it (diffusion or free-streaming out).

During the collapse huge quantities of neutrinos are generated. These ones transport thermal energy from the most interior regions to the exterior layers [9,10,12]. Because of the high densities and temperature, the neutrinos interact with matter. In their trip toward the surface they get thermalized and drive the star to a new equilibrium state. The most important thermalization processes are the absorption of neutrinos by neutrons and collisions between neutrinos and electrons. Consequently we have chosen a density range according to these interactions ($\rho_c \sim 10^{15} \text{ g cm}^{-3}$, $\rho_a \sim 10^{12} \text{ g cm}^{-3}$), allowing us to treat the radiation in the diffusive limit.

The density and pressure profile in the central layers vary little during the collapse. Therefore, the behavior of the zones nearby the surface is perhaps the most important. Due to the decrease, in these layers, of the pressure gradient with respect to the surface, the velocity of collapse of the former is larger than the corresponding to this one. This behavior also occurs in models with a density at the surface of about $10^{14} \text{ g cm}^{-3}$, though then the effect is not so intense. Also, the final radius of the star depends on the density at the surface. The higher initial energy density at the surface, the larger final radius. As previously mentioned, the largest variations in energy density occur at the surface. This effect is probably due to the importance of the radiation in the evolution of the neutrinosphere. In that zone, the heat flow is

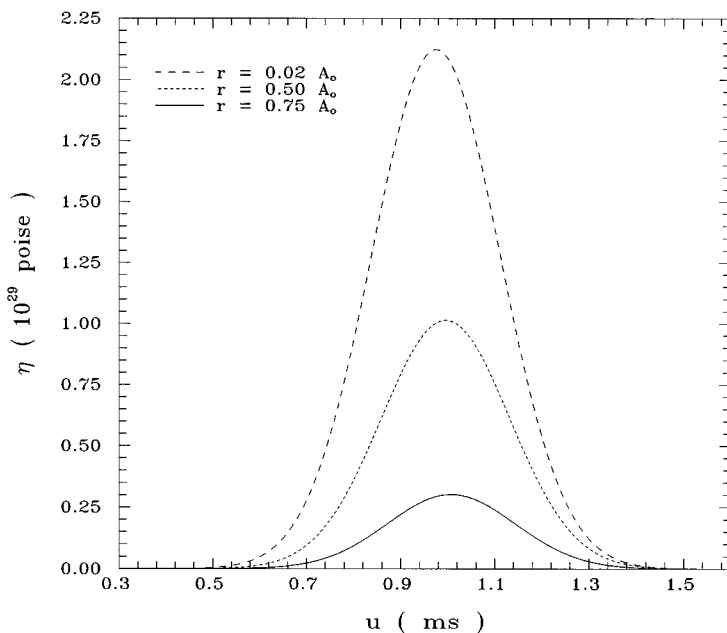


FIG. 10. Evolution of the shear viscous coefficient η .

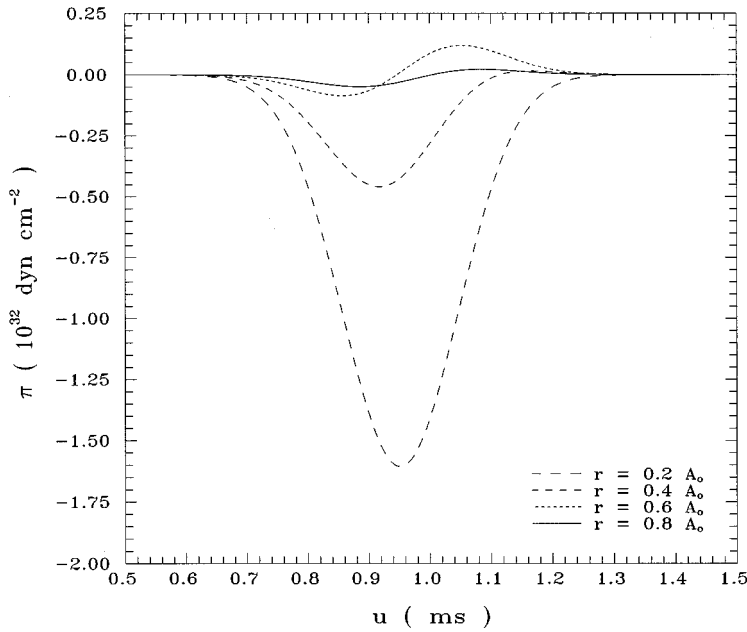


FIG. 11. Evolution of the shear viscous pressure in different layers of the star.

much weaker than in the inner regions. Nevertheless, it is possible that the radiation energy density in it comprises a large part of total energy density.

The knowledge of the temperature of the star is the key to establish which processes can take place in its bosom. At the variance with the heat flow, this quantity cannot be obtained from Einstein's equations. It is absolutely necessary then to appeal to some thermodynamic theory of irreversible processes. We have taken a further step with respect to other analysis by introducing the EIT in its covariant formulation [16,17], avoiding in this way the unphysical behavior of the conventional theory [13]. The rigorous study of transport equations derived from EIT is technically complex. Therefore, we have appealed to the so-called "truncated" form that reduces to the Maxwell-Cattaneo equations [21]. To

solve the corresponding equation for temperature we have found the mean free time of the neutrinos. In so doing we have considered both reactions mentioned above, if the neutrinos are generated by thermal emission with energy near $k_B T$. In this way it is possible to establish the dependence of the thermal conductivity coefficient on temperature ($\chi \propto T^{3/2}$). Then, solving the equation for the evolution of the heat flow, we found the temperature. Also we have solved the classic transport equation, finding out considerable differences in the neutrinosphere between both theories. These temperatures disagree from one another in the first and last stages of the collapse.

It is worth emphasizing a peculiarity of the temperature in the innermost layers. This one is insensitive in that zone to the boundary condition imposed on the surface. Therefore,

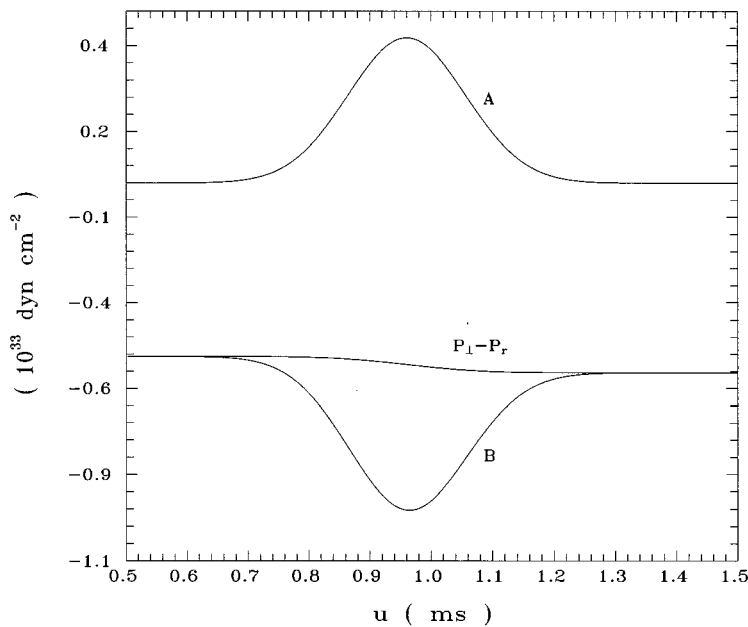


FIG. 12. Comparative plot of the different contributions to the anisotropy (2.19) at $r = 0.1 A_0$. Lines marked A and B correspond to terms $-3\pi/2$ and μ , respectively.

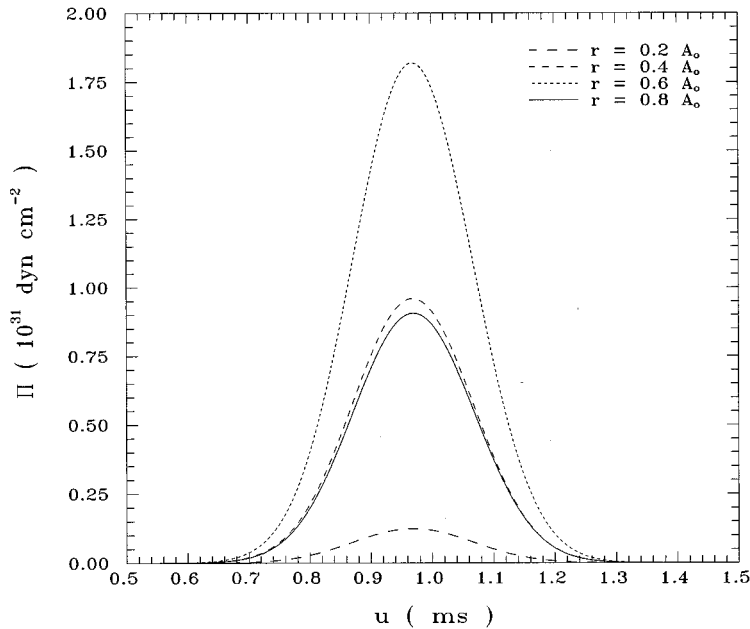


FIG. 13. Evolution of the bulk viscous pressure within the star.

those neutrinos that manage to escape from the star lack information about the temperature of the central regions, in other words their energy in the surface is not correlated with that of the interior. This suggests that these have been created in a region close to the surface, the so-called neutrinosphere ([9], p. 586, [38], p. 295, [49], p. 17). The neutrinosphere is commonly associated with the effective temperature, T_{eff} , which coincides with the material temperature in its lower limit. Through the introduction of T_{eff} we find out the temperature at the surface. Thus, we have obtained a credible boundary condition for the heat transport equation. We have supposed, therefore, that the layers of the star that are sensitive to a change in the boundary condition form the neutrinosphere with a thickness of 500–700 m. This length approximately coincides with the neutrino mean free path in that zone. This fact reinforces the hypothesis that the emergent neutrinos have been created in the interior region that delimits the neutrinosphere.

Once the temperature was found, we went on by solving the transport equations of the remaining dissipative flows (bulk and shear viscous pressure). Using Weinberg expressions [8] for the viscosity coefficients and expression (3.17), we have obtained $\zeta, \eta \propto T^{5/2}$. This yields a value about 10^{29} poise for shear viscosity coefficient. This value is much larger than the corresponding for interactions among electrons, protons, and neutrons. Although ζ can be of the same order that η , the value we have obtained for ζ is about 100 times lower than η . This is because we have assumed the center of the star as an ultrarelativistic Fermi gas and it implies an equation of state of the form $P = \rho/3$. It is well known that for a fluid governed by this equation the bulk

viscosity coefficient vanishes [8]. Though throughout the star this limit is not strictly fulfilled, the relationship between the radial pressure and energy density restricts the value of ζ . In spite of this, from 7 km of the center upward the bulk viscous pressure is comparable to a shear one. In an anisotropic model, shear viscous pressure is restricted by the difference between the tangential and radial pressures. Therefore, one can expect that its contribution to the total pressure is small. It is worth noting the contribution of shear viscous pressure to the anisotropy. According to the model studied here, it seems that the viscosity is responsible for an important part of the inner anisotropy. Then, the shear viscous pressure greatly contributes to total anisotropy in approximately the two nearest kilometers to the center of the star. It is certain that in the most internal zone of the star the anisotropy is less important than in the peripheral region. Though, under certain circumstances (larger collapse speeds) the importance of viscous pressure in connection to the anisotropy will be extended to more afar zones.

ACKNOWLEDGMENTS

I would like to thank the staff of the Laboratorio de Física Teórica de la Universidad de Los Andes (Mérida, Venezuela) for their hospitality, especially to Luís Núñez for bringing [25] to my attention and for useful discussions at different stages of this work. Also Diego Pavón is acknowledged for his encouragement and advice. This work was partially supported by the Programa de Formación Científico de la Universidad de Los Andes (Mérida, Venezuela) and by the Spanish Ministry of Education under Grant No. PB94-0718.

[1] V. Canuto, *Am. Rev. Astron. Astrophys.* **12**, 167 (1974).
 [2] R.I. Bowers and E.P.T. Liang, *Astrophys. J.* **188**, 657 (1974).
 [3] L. Herrera and N.O. Santos, *Phys. Rep.* (to be published).

[4] L. Herrera, J. Jiménez, and W. Barreto, *Can. J. Phys.* **67**, 855 (1989).
 [5] W. Barreto and S. Rojas, *Astron. Sp. Sci.* **193**, 201 (1992).

- [6] J. Martínez, D. Pavón, and L.A. Núñez, *Mon. Not. R. Astron. Soc.* **271**, 463 (1994).
- [7] L. Herrera, J. Jiménez, and G.J. Ruggeri, *Phys. Rev. D* **22**, 2305 (1980).
- [8] S. Weinberg, *Astrophys. J.* **168**, 175 (1971).
- [9] S.L. Shapiro and S.A. Teukolsky, *Black Holes, White Dwarfs and Neutron Stars* (Wiley, New York, 1983).
- [10] S.W. Bruenn, *Astrophys. J. Suppl. Ser.* **58**, 771 (1985).
- [11] M. Demiański, in *Relativistic Astrophysics*, International Series in Nat. Phyl. Vol. 110, edited by D. Ter Haar (Pergamon, Oxford, 1985).
- [12] J.N. Bahcall, *Neutrino Astrophysics* (Cambridge University Press, Cambridge, England, 1989).
- [13] C. Eckart, *Phys. Rev.* **58**, 919 (1940).
- [14] G.A. Kluitenberg, S.R. de Groot, and P. Mazur, *Physica* **19**, 689 (1953).
- [15] L.D. Landau and E.M. Lifshitz, *Mécanique des Fluides* (MIR, Moscou, 1971).
- [16] W. Israel, *Ann. Phys. (N.Y.)* **100**, 310 (1976).
- [17] D. Pavón, D. Jou, and J. Casas-Vázquez, *Ann. Inst. Henri Poincaré Sec. A* **36**, 79 (1982).
- [18] D. Pavón, J. Bafaluy, and D. Jou, *Class. Quantum Grav.* **8**, 347 (1991).
- [19] M.O. Calvão and J.M. Salim, *Class. Quantum Grav.* **9**, 127 (1992).
- [20] V. Romano and D. Pavón, *Phys. Rev. D* **47**, 1396 (1993).
- [21] D. Jou, J. Casas-Vázquez, and G. Lebon, *Extended Irreversible Thermodynamics* (Springer, Berlin, 1993).
- [22] W.A. Hiscock and L. Lindblom, *Ann. Phys. (N.Y.)* **151**, 466 (1983).
- [23] J. Triginer and D. Pavón, *Class. Quantum Grav.* **12**, 689 (1995).
- [24] A. Di Prisco, L. Herrera, and M. Esculpi, *Class. Quantum Grav.* **13**, 1053 (1996).
- [25] M.K. Gokhroo and A.L. Mehra, *Gen. Relativ. Gravit.* **26**, 75 (1994).
- [26] H. Bondi, M.G.J. van der Burg, and A.W.K. Metzner, *Proc. R. Soc. London* **A269**, 21 (1962).
- [27] H. Bondi, *Proc. R. Soc. London* **A281**, 39 (1964).
- [28] P.C. Vaidya, *Proc. Ind. Acad. Sci. Sect. A* **33**, 264 (1951).
- [29] R.W. Lindquist, *Ann. Phys. (N.Y.)* **37**, 487 (1966).
- [30] D. Mihalas and B. Mihalas, *Foundations of Radiation Hydrodynamics* (Oxford University Press, Oxford, 1984).
- [31] L. Herrera and J. Jiménez, *Phys. Rev. D* **28**, 2987 (1983).
- [32] N.O. Santos, *Mon. Not. R. Astron. Soc.* **216**, 403 (1985).
- [33] L. Herrera and L.A. Núñez, *Fundam. Cosmic Phys.* **14**, 235 (1990).
- [34] M. Cosenza, L. Herrera, M. Esculpi, and L. Witten, *J. Math. Phys.* **22**, 118 (1981).
- [35] M. Cosenza, L. Herrera, M. Esculpi, and L. Witten, *Phys. Rev. D* **25**, 2527 (1982).
- [36] R. Kippenhan and A. Weigert, *Stellar Structure and Evolution* (Springer-Verlag, Berlin, 1990).
- [37] A. Burrows and J.M. Lattimer, *Astrophys. J.* **307**, 178 (1986).
- [38] C.J. Hansen and S.D. Kawaler, *Stellar Interiors Physical Principles, Structure, and Evolution* (Springer, New York, 1994).
- [39] F. Halzen and A.D. Martin, *Quarks and Leptons, an Introductory Course in Modern Particle Physics* (Wiley, New York, 1983).
- [40] S.S. Bayin, *Phys. Rev. D* **26**, 6 (1982).
- [41] J. Ponce de León, *Gen. Relativ. Gravit.* **19**, 797 (1987).
- [42] J. Ponce de León, *J. Math. Phys.* **28**, 1114 (1987).
- [43] J. Ponce de León, *Phys. Rev. D* **35**, 2060 (1987).
- [44] S.D. Maharaj and R. Maartens, *Gen. Relativ. Gravit.* **21**, 899 (1989).
- [45] G. Börner, *On the Properties of Matter in Neutron Stars*, Springer Tracts in Physics (Springer, Berlin, 1973).
- [46] Ch.A. Kolassis, N.O. Santos, and D. Tsoubelis, *Class. Quantum Grav.* **5**, 1329 (1988).
- [47] E. Flowers and N. Itoh, *Astrophys. J.* **230**, 847 (1979).
- [48] E. Flowers and N. Itoh, *Astrophys. J.* **206**, 218 (1976).
- [49] H. Chiu, *Stellar Physics* (Blaisdell, New York, 1968).